

Diamagnetism in disordered graphene

Mikito Koshino and Tsuneya Ando

Department of Physics, Tokyo Institute of Technology 2-12-1 Ookayama, Meguro-ku, Tokyo 152-8551, Japan

(Dated: February 1, 2008)

The orbital magnetism is studied in graphene monolayer within the effective mass approximation. In models of short-range and long-range disorder, the magnetization is calculated with self-consistent Born approximation. In the zero-field limit, the susceptibility becomes highly diamagnetic around zero energy, while it has a long tail proportional to the inverse of the Fermi energy. We demonstrated how the magnetic oscillation vanishes and converges to the susceptibility, on going from a strong-field regime to zero-field. The behavior at zero energy is shown to be highly singular.

I. INTRODUCTION

The monolayer graphene has a band structure analogous to the massless relativistic particle, and its peculiar electronic properties have attracted much interest. Recently several experimental techniques make atomically thin graphene sheets available,^{1,2,3,4} and the nature of this unique system is being revealed. In this paper we present a theoretical study on the orbital magnetism of graphene including the disorder effects.

The graphene has a semi-metallic electronic structure where the conduction and valence bands touch at the Brillouin zone corners, K and K' points. Around the band touching point (set to $\varepsilon = 0$), the low energy spectrum has a linear dispersion analogous to the massless Dirac Fermion. The spectrum in a magnetic field is different from that in usual metals in that the Landau level spacing is not even but wider in lower energies, and is proportional to \sqrt{B} , not to B , where B is the magnetic field,⁵ and this leads to an unusual behavior in the orbital magnetization. The magnetism of graphene was first studied as a simple model for three-dimensional (3D) graphite,⁵ where the susceptibility of the disorder-free graphene was calculated within the effective mass approximation. It was found that the system exhibits a large diamagnetism at $\varepsilon_F = 0$, expressed as a delta function of ε_F at the absolute zero temperature. The graphene magnetism was considered again in studies on the graphite intercalation compounds, where the tight-binding model was applied for a wide range of Fermi energies.^{6,7,8,9}

In the presence of the disorder, it becomes nontrivial how the magnetization behaves under this unusual electronic structure. Particularly, it is not clear how the delta-function in the susceptibility is broadened, since we naively suppose that the scattering is absent at $\varepsilon = 0$ where the density of states vanishes. Moreover, we do not know how the magnetic oscillation is destroyed by the disorder when we go from the high-field to the low-field regime, and how it converges to the zero-field limit.

The effects of disorder on graphene under magnetic fields have been examined in early theoretical studies before the experimental discovery of graphene, where the electronic structure,¹⁰ the transport properties,^{10,11,12} and the de Haas-van Alphen effect¹³ were investigated.

More recently the Shubnikov-de Haas oscillation was studied in disordered graphene,^{14,15} and the spectral and transport properties were examined in presence of lattice defects under magnetic fields.¹⁶

The purpose of this paper is to calculate the magnetization of disordered graphene in arbitrary magnetic fields, and to obtain the perspective which connects the high-field and zero-field limit. For the model disorder, we introduce the short-ranged and long-ranged scatterers following the formulation in Ref. 10,11,12, and treat the disorder effects within a self-consistent Born approximation (SCBA). The paper is organized as follows: In Sec. II we briefly discuss the effective mass Hamiltonian and the SCBA in order to make this paper self-contained although fully discussed previously.¹⁰ The analytic discussions of the magnetization in the zero-field limit and the numerical calculation for finite fields are presented in Sec. III. Discussions and conclusions are given in Sec. IV.

II. FORMULATION

A. Hamiltonian

We start with the effective mass Hamiltonian in an ideal graphene in a magnetic field given by¹⁰

$$\mathcal{H}_0 = \frac{\gamma}{\hbar} \begin{pmatrix} 0 & \pi_x - i\pi_y & 0 & 0 \\ \pi_x + i\pi_y & 0 & 0 & 0 \\ 0 & 0 & 0 & \pi_x + i\pi_y \\ 0 & 0 & \pi_x - i\pi_y & 0 \end{pmatrix}, \quad (1)$$

where $\boldsymbol{\pi} = \mathbf{p} + e\mathbf{A}$ with the electron momentum operator \mathbf{p} and the vector potential $\mathbf{A} = (0, Bx)$ in the Landau gauge, and $\gamma = \sqrt{3}a\gamma_0/2$ with a being the lattice constant and γ_0 the hopping integral between nearest-neighbor carbon atoms. A graphene is composed of a honeycomb network of carbon atoms, where a unit cell contains a pair of sublattices, denoted by A and B . The Hamiltonian (1) operates on a four-components wave function $(F_A^K, F_B^K, F_A^{K'}, F_B^{K'})$, where F_A^K and F_B^K represent the envelope functions at A and B sites for K point, respectively, and $F_A^{K'}$ and $F_B^{K'}$ for K' .

The eigenstates are labeled by (j, n, k) with the valley index $j = K, K'$, the Landau level index $n = 0, \pm 1, \dots$,

and the wave vector k along y direction.¹⁰ The eigenenergy depends solely on n as $\varepsilon_n = \hbar\omega_B \operatorname{sgn}(n)\sqrt{|n|}$, where $\hbar\omega_B = \sqrt{2}\gamma/l$ with $l = \sqrt{\hbar/eB}$. The wave functions are written as

$$\mathbf{F}_{nk}^K = \frac{C_n}{\sqrt{L}} \exp(iky) \begin{pmatrix} \operatorname{sgn}(n)(-i)\phi_{|n|-1,k} \\ \phi_{|n|,k} \\ 0 \\ 0 \end{pmatrix}, \quad (2)$$

$$\mathbf{F}_{nk}' = \frac{C_n}{\sqrt{L}} \exp(iky) \begin{pmatrix} 0 \\ 0 \\ \phi_{|n|,k} \\ \operatorname{sgn}(n)(-i)\phi_{|n|-1,k} \end{pmatrix}, \quad (3)$$

where $\phi_{n,k}(x) = (2^n n! \sqrt{\pi l})^{-1/2} e^{-z^2/2} H_n(z)$, with $z = (x + kl^2)/l$ and H_n being the Hermite polynomial, and

$$C_n = \begin{cases} 1 & (n = 0), \\ 1/\sqrt{2} & (n \neq 0), \end{cases} \quad (4)$$

$$\operatorname{sgn}(n) = \begin{cases} 0 & (n = 0), \\ n/|n| & (n \neq 0). \end{cases}$$

For the disorder potential, we consider two simple models: short- and long-ranged scatterers.¹⁰ The first is on-site potential localized at a particular A or B sites with a random amplitude. A scatterer on A site at \mathbf{R}_A is represented as

$$U(\mathbf{r}) = \begin{pmatrix} 1 & 0 & z_A^* z'_A & 0 \\ 0 & 0 & 0 & 0 \\ z_A z'^*_A & 0 & 1 & 0 \\ 0 & 0 & 0 & 0 \end{pmatrix} u_i \delta(\mathbf{r} - \mathbf{R}_A), \quad (5)$$

and that for B site at \mathbf{R}_B as

$$U(\mathbf{r}) = \begin{pmatrix} 0 & 0 & 0 & 0 \\ 0 & 1 & 0 & z_B^* z'_B \\ 0 & 0 & 0 & 0 \\ 0 & z_B z'^*_B & 0 & 1 \end{pmatrix} u_i \delta(\mathbf{r} - \mathbf{R}_B), \quad (6)$$

where we introduced $z_X = e^{i\mathbf{K} \cdot \mathbf{R}_X}$, $z'_X = e^{i\mathbf{K}' \cdot \mathbf{R}_X}$ with $X = A$ and B , and $u_i = (\sqrt{3}a^2/2)U_i$ with the on-site energy U_i . We assume that the scatterers are equally distributed on A and B sites with density $n_i^A = n_i^B = n_i/2$ and the mean square amplitude $\langle (u_i^A)^2 \rangle = \langle (u_i^B)^2 \rangle = u_i^2$.

Dominant scatterers in graphenes are expected to have their potential range larger than the lattice constant for which inter-valley scattering is much smaller than intra-valley scattering. Further, realistic scatterers are likely to have the range comparable to the Fermi wavelength.^{20,21,22} In the following, however, we shall assume scatterers with potential range smaller than the Fermi wavelength. The reason is that the results are expected to remain qualitatively the same and further that actual calculations are practically possible.

In this long-range model, a scatterer at \mathbf{R} is expressed by

$$U(\mathbf{r}) = \begin{pmatrix} 1 & 0 & 0 & 0 \\ 0 & 1 & 0 & 0 \\ 0 & 0 & 1 & 0 \\ 0 & 0 & 0 & 1 \end{pmatrix} u_i \delta(\mathbf{r} - \mathbf{R}). \quad (7)$$

We assume the scatterer density n_i and the mean square amplitude u_i^2 . It was shown that the transport properties in the short-ranged disorder and the long-ranged one are qualitatively similar.^{10,11,12}

B. Self-Consistent Born Approximation (SCBA)

We introduce the self-consistent Born approximation for graphene, following the formulation in Ref. 10. The self-energy of the disorder-averaged Green's function $\langle G_{\alpha,\alpha'} \rangle$ is given by

$$\Sigma_{\alpha,\alpha'}(\varepsilon) = \sum_{\alpha_1, \alpha'_1} \langle U_{\alpha,\alpha_1} U_{\alpha'_1,\alpha'} \rangle \langle G_{\alpha_1,\alpha'_1}(\varepsilon) \rangle, \quad (8)$$

with $\alpha = (j, n, k)$, where $\langle \dots \rangle$ represents the average over the impurity configurations.

In the short-range model, the self-energy and thus the averaged Green's function become diagonal with respect to α , and further, the self-energy is independent of α . We then have

$$\langle G_{\alpha,\alpha'}(\varepsilon) \rangle = \delta_{\alpha,\alpha'} G_\alpha(\varepsilon), \quad (9)$$

$$G_\alpha(\varepsilon) = \frac{1}{\varepsilon - \varepsilon_\alpha - \Sigma(\varepsilon)}, \quad (10)$$

where $\Sigma(\varepsilon)$ is the self-energy. The self-consistent equation (8) is explicitly written as

$$\Sigma(\varepsilon) = \frac{W(\hbar\omega_B)^2}{2} \sum_{n=-\infty}^{\infty} \frac{g(\varepsilon_n)}{\varepsilon - \varepsilon_n - \Sigma(\varepsilon)}, \quad (11)$$

where we introduced a cutoff function $g(\varepsilon)$ which is 1 in $|\varepsilon| \ll \varepsilon_c$ and smoothly vanishes around $\varepsilon = \pm \varepsilon_c$. For example we can take $g(\varepsilon) = \varepsilon_c^\alpha / (|\varepsilon|^\alpha + \varepsilon_c^\alpha)$ with $\alpha \geq 2$. Further, W is the dimensionless parameter for the disorder strength defined as

$$W = \frac{n_i u_i^2}{4\pi\gamma^2}. \quad (12)$$

The density of states per a unit area is given by

$$\rho(\varepsilon) = -\frac{g_v g_s}{2\pi^2 \gamma^2 W} \operatorname{Im} \Sigma(\varepsilon + i0), \quad (13)$$

where $g_v = g_s = 2$ is the valley and spin degeneracy, respectively.

In the zero-field limit, (11) becomes

$$\Sigma(\varepsilon) = 2W \int_0^\infty t dt \frac{(\varepsilon - \Sigma)g(t)}{(\varepsilon - \Sigma)^2 - t^2}. \quad (14)$$

The integral is approximately written in $\varepsilon \ll \varepsilon_c$ as

$$\Sigma(\varepsilon) = -W(\varepsilon - \Sigma) \log \left(-\frac{\varepsilon_c^2}{(\varepsilon - \Sigma)^2} \right), \quad (15)$$

where the branch of log must be appropriately chosen. Then we can solve this equation analytically,

$$\Sigma(\varepsilon) = \varepsilon - \varepsilon \left[2W f_L \left(-\frac{i\varepsilon}{2W\Gamma_0} \right) \right]^{-1}. \quad (16)$$

where $f_L(z)$ is the Lambert W-function, which is defined as the inverse function of $z = ye^y$, and

$$\Gamma_0 = \varepsilon_c \exp \left(-\frac{1}{2W} \right). \quad (17)$$

At $\varepsilon = 0$ in particular, we have

$$\Sigma(0 + i0) = -i\Gamma_0. \quad (18)$$

In $|\varepsilon| \gg \Gamma_0$, Σ is approximately written with use of the expansion $f_L(z) \approx \log(z) - \log \log(z)$ for $|z| \gg 1$ as,

$$\Sigma(\varepsilon + i0) \approx -2W\varepsilon \log \left| \frac{\varepsilon_c}{\varepsilon} \right| - i\pi W|\varepsilon|. \quad (19)$$

This can be alternatively derived from (14) with assuming $|\varepsilon| \gg |\Sigma|$, and thus corresponds to the Boltzmann limit. If $W \sim 1$, the states around $\varepsilon = \varepsilon_c$ are completely mixed up with those at $\varepsilon = 0$, as expected from the imaginary part of Σ in (19). To avoid this undesirable situation, we assume $W \ll 1$ in the following calculation.

When the magnetic field is large enough that a Landau level is well separated from others, (11) can be approximately solved around the energy of that level. The width of the Landau level is estimated as 2Δ with

$$\Delta = \sqrt{2W}\hbar\omega_B. \quad (20)$$

In the long-ranged model, the self-energy and Green's function have off-diagonal matrix elements between (j, n, k) and $(j, -n, k)$. We have

$$\Sigma_{\alpha,\alpha'}(\varepsilon) = \delta_{j,j'}\delta_{k,k'}[\delta_{n,n'}\Sigma^d(\varepsilon) + \delta_{n,-n'}\Sigma^o(\varepsilon)], \quad (21)$$

Introducing $\Sigma^\pm \equiv \Sigma^d \pm \Sigma^o$, the equation becomes

$$\Sigma^+(\varepsilon) = W(\hbar\omega_B)^2 \sum_{n=0}^{\infty} \frac{(\varepsilon - \Sigma^-)g(\varepsilon_n)}{(\varepsilon - \Sigma^+)(\varepsilon - \Sigma^-) - \varepsilon_n^2}, \quad (22)$$

$$\Sigma^-(\varepsilon) = W(\hbar\omega_B)^2 \sum_{n=1}^{\infty} \frac{(\varepsilon - \Sigma^+)g(\varepsilon_n)}{(\varepsilon - \Sigma^+)(\varepsilon - \Sigma^-) - \varepsilon_n^2}, \quad (23)$$

with the same W as the short-range case Eq. (12). The density of states per a unit area becomes

$$\rho(\varepsilon) = -\frac{g_v g_s}{2\pi^2 \gamma^2 W} \frac{1}{2} \text{Im} [\Sigma^+(\varepsilon + i0) + \Sigma^-(\varepsilon + i0)]. \quad (24)$$

In a high magnetic field such that Landau levels are well separated, the width of the Landau level becomes the same as Δ in (20) for the level $N \neq 0$, while it is $\sqrt{2}\Delta$ for $N = 0$. In the weak-field limit, Σ^+ and Σ^- coincide and satisfy (14).

C. Magnetization and susceptibility

The magnetization is defined as

$$M = - \left(\frac{\partial \Omega}{\partial B} \right)_\mu, \quad (25)$$

where $\Omega(T, \mu, B)$ is the thermodynamic potential and μ is the chemical potential. By noting that the electron concentration N is given by

$$N = - \left(\frac{\partial \Omega}{\partial \mu} \right)_B, \quad (26)$$

we obtain so-called Maxwell's relation,

$$\left(\frac{\partial M}{\partial \mu} \right)_B = \left(\frac{\partial N}{\partial B} \right)_\mu. \quad (27)$$

We write N in terms of the density of states ρ as

$$N = \int_{-\infty}^{\infty} \rho(\varepsilon, B) f(\varepsilon) d\varepsilon, \quad (28)$$

with $f(\varepsilon) = 1/(1 + e^{(\varepsilon - \mu)/k_B T})$, and calculate M by integrating (27) over μ . After a little algebra, we obtain

$$M = \int_{-\infty}^{\infty} d\varepsilon f(\varepsilon) \int_{-\infty}^{\varepsilon} d\varepsilon' \frac{\partial \rho(\varepsilon', B)}{\partial B}. \quad (29)$$

In SCBA, we evaluate this by substituting ρ with (13) or (24) depending on the type of the disorder. The magnetization in a nonzero temperature is always written in terms of that of $T = 0$ as

$$M(T, \mu) = \int_{-\infty}^{\infty} d\varepsilon \left(-\frac{\partial f(\varepsilon)}{\partial \varepsilon} \right) M(0, \varepsilon). \quad (30)$$

The magnetic susceptibility is given by

$$\chi = \left. \frac{\partial M}{\partial B} \right|_{B=0}, \quad (31)$$

taking the zero-field limit in (29).

III. MAGNETIZATION IN DISORDERED GRAPHENES

For the short-ranged disorder, Eqs. (11), (13), and (29) lead to the expression

$$\chi = -\frac{g_v g_s}{6\pi^2} \frac{e^2 \gamma^2}{\hbar^2} \int_{-\infty}^{\infty} d\varepsilon f(\varepsilon) \text{Im} \frac{1}{(\varepsilon - \Sigma(\varepsilon))^2}, \quad (32)$$

where Σ is the self-energy at $B = 0$. The derivation of this is straightforward and is presented in Appendix A.

In the energy range $\varepsilon \ll \varepsilon_c$, we can use the explicit form (16) for Σ . At absolute zero temperature, we execute the integral to have

$$\chi(\varepsilon_F) = -\frac{g_v g_s}{3\pi^2} \frac{e^2 \gamma^2}{\hbar^2} \frac{2W}{\Gamma_0} F \left(\frac{\varepsilon_F}{2W\Gamma_0} \right), \quad (33)$$

with

$$F(x) = -\frac{1}{x} \text{Im} \left[f_L(-ix) + \frac{1}{2} f_L^2(-ix) \right]. \quad (34)$$

The function $F(x)$ has the maximum at $x = 0$ with $F(0) = 1$, giving

$$\chi(0) = -\frac{g_v g_s}{3\pi^2} \frac{e^2 \gamma^2}{\hbar^2} \frac{2W}{\Gamma_0}. \quad (35)$$

In the energy range $|\varepsilon| \gg \Gamma_0$, we use (19) and obtain

$$\chi(\varepsilon_F) \approx -\frac{g_v g_s}{3\pi} \frac{e^2 \gamma^2}{\hbar^2} \frac{W}{|\varepsilon_F|}, \quad (36)$$

which monotonically decreases as $|\varepsilon_F|$ increases. The behavior of $\chi(\varepsilon_F)$ can be roughly described as a long-tailed peak (36) which saturates around $\varepsilon \sim \Gamma_0$ to the value (35).

When the disorder W becomes smaller, the peak of the susceptibility (33) becomes narrower and higher as Γ_0 behaves as $\propto \exp(-1/2W)$. The integral over ε rigorously becomes $-g_v g_s e^2 \gamma^2 / (6\pi \hbar^2)$, as proved in Appendix A. This is roughly verified by integrating (36) from $-\varepsilon_c$ to ε_c with the region $|\varepsilon| < \Gamma_0$ excluded and by using Eq. (17). Thus, in the clean limit $W \rightarrow 0$, χ becomes a delta function,

$$\chi(\varepsilon_F) = -\frac{g_v g_s}{6\pi} \frac{e^2 \gamma^2}{\hbar^2} \delta(\varepsilon_F), \quad (37)$$

which agrees with the result in Refs. 5 and 7.

For the long-ranged disorder, the expression for the susceptibility in $|\varepsilon| \ll \varepsilon_c$ becomes,

$$\begin{aligned} \chi \approx & -\frac{g_v g_s}{6\pi^2} \frac{e^2 \gamma^2}{\hbar^2} \int_{-\infty}^{\infty} d\varepsilon f(\varepsilon) \\ & \times \text{Im} \frac{1}{X^2} \left[1 - \frac{3W}{1 + W \log(-\varepsilon_c^2/X^2)} \right], \end{aligned} \quad (38)$$

with $X = \varepsilon - \Sigma(\varepsilon)$. The derivation is given in Appendix A. Compared with the short-ranged case (32), we have the extra second term of the order of $O(W)$, but this gives a minor effect since W is assumed to be small. When $O(W^2)$ is neglected, the susceptibility becomes just $1 - 3W$ times as large as in the short-ranged disorder. Accordingly the integration of χ over ε weakly depends on W , while in $W \rightarrow 0$ we again get (37).

In a strong magnetic field where the Landau levels are resolved, the magnetization exhibits an oscillatory behavior as a function of the Fermi energy and the magnetic field. The damping of the magnetic oscillation in the disorder was discussed in a simple approximation where the scattering rate was assumed to be constant.¹³ We calculate here the magnetization at nonzero fields in SCBA, since this kind of treatment is essential in investigating the behavior at the zero energy. We numerically evaluate (29), in which the derivative in B is taken with a finite increment ΔB . Here and the following we take

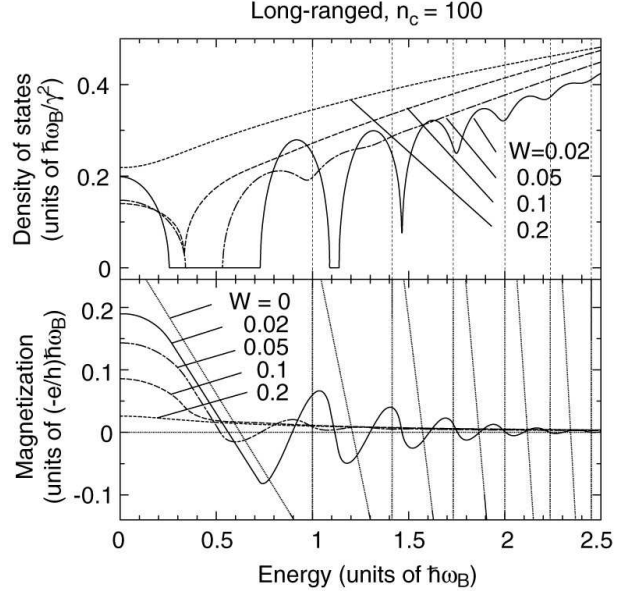


FIG. 1: Density of states (above) and the magnetization at $T = 0$ (below) in the long-ranged disorder with several strength W 's. The plot is against the Fermi energy, and the values are per a spin and per a valley. Vertical dashed lines shows the energies of the Landau level in the clean limit.

the long-ranged disorder, and plot every quantity per a spin and a valley. The field amplitude B is specified by $n_c = (\varepsilon_c/\hbar\omega_B)^2 \propto 1/B$, which represents how many Landau levels are accommodated between $\varepsilon = 0$ and ε_c . We set $n_c = 100$ here.

As an overview of the dependence on the disorder strength, we plot in Fig. 1 the density of states and the magnetization for several W 's at zero temperature and a fixed magnetic field. The density of states is basically equivalent to that already obtained in Ref. 10, but we present this here to demonstrate the relation to the magnetization. We see that the Landau levels are separated more clearly in the lower energy due to the larger level splitting, and the magnetization exhibits an oscillation in the corresponding region. As W becomes larger, the oscillatory part vanishes from the higher-energy side. The results for the short-range disorder are not shown, but qualitatively similar to those for the long-range disorder.

The Landau level broadening in disordered graphene has also been studied for a system with lattice vacancies.¹⁶ The result becomes somewhat different from our model in that the Landau levels around $\varepsilon = 0$ become much broader than higher levels, in accordance with the fact that the vacancies give rise to impurity states around the band touching point.^{16,17,18,19} We do not have a strong scattering enhancement at $\varepsilon = 0$ in the present effective-mass model, where the on-site energy of the disorder potential is assumed to be much smaller than the π -band width.

We focus on the case of $W = 0.02$ and show in Fig.

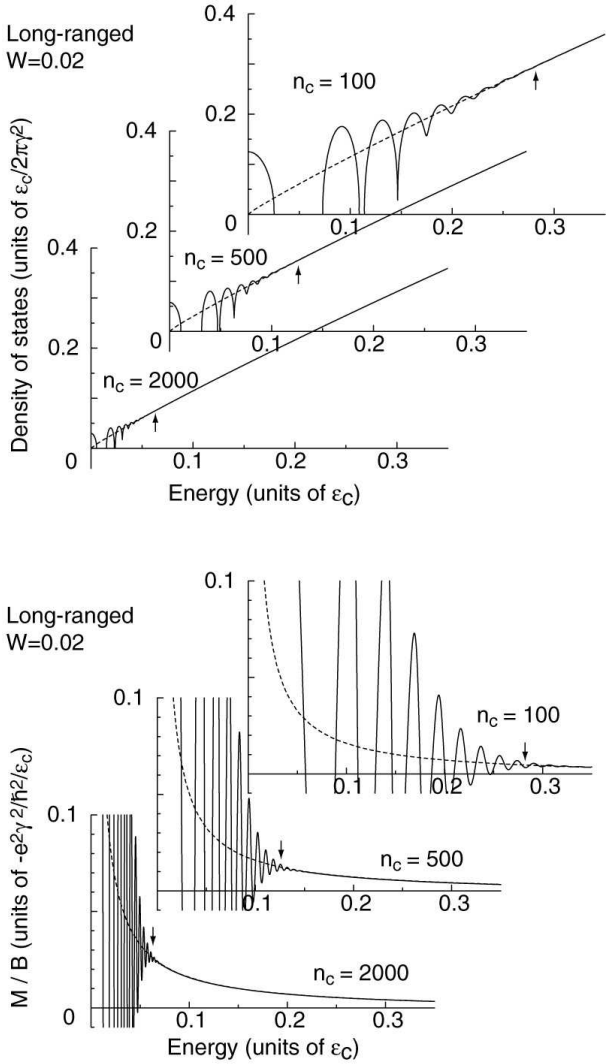


FIG. 2: Density of states (above) and the magnetization at $T = 0$ (below) in the long-ranged disorder with $W = 0.02$, in several magnetic fields specified by $n_c = (\varepsilon_c/\hbar\omega_B)^2$. Dashed curves show the zero-field limit.

2 the plots of the density of states and of M/B for several different magnetic fields. We see that the oscillation in M terminates at a certain point and in higher ε M/B sticks to the zero-field limit χ shown as a dashed line. The oscillation is observable when the Landau level spacing $\hbar\omega_B|\sqrt{n+1}-\sqrt{n}|\sim(\hbar\omega_B)^2/(2|\varepsilon|)$ is larger than the energy broadening at $B=0$, which is $\pi W|\varepsilon|$ in the Boltzmann limit (19). Then the condition becomes

$$\varepsilon > \frac{\hbar\omega_B}{\sqrt{2\pi W}}. \quad (39)$$

In Fig. 2, the boundary is indicated by an arrow, which actually divides the oscillating and non-oscillating parts.

We show in Fig. 3 the renormalized density of states and magnetization against $\varepsilon/\hbar\omega_B$. We can see that the Landau level width is almost independent of the magnetic

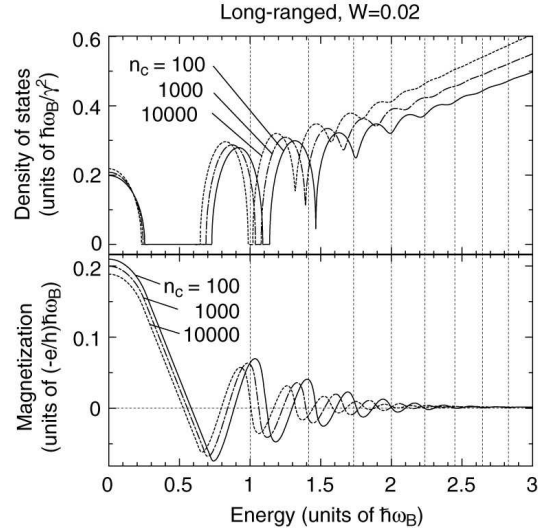


FIG. 3: Density of states (above) and the magnetization at $T = 0$ (below) in the long-ranged disorder with $W = 0.02$, in several magnetic fields. The vertical and horizontal axes are renormalized in units of factors $\propto \hbar\omega_B$. Dashed vertical lines are the energies of the Landau levels in the ideal limit.

field in this scale, as expected from (20) in the strong-field limit, while each level shifts toward zero energy as B becomes smaller (n_c larger). From the real part of Σ in (19), the shift can be estimated as $\Delta\varepsilon_n \sim -W\varepsilon_n \log |n_c/n|$. The amplitude of the magnetic oscillation roughly scales as $M \propto \hbar\omega_B \propto \sqrt{B}$, in contrast to the behavior in the non-oscillating region where the relation $M = \chi B$ is valid. This is because the gain of the total energy U due to the magnetic field is proportional both to the Landau level spacing ($\propto \sqrt{B}$) and the level degeneracy ($\propto B$), which gives $M \sim -dU/dB \propto \sqrt{B}$.⁵ The oscillation amplitude gradually reduces as B becomes smaller, as the level shift causes reduction of the energy gap.

We expect that the lowest Landau gap vanishes when the gap width is as small as the energy broadening at $\varepsilon = 0$ in zero field, or

$$\hbar\omega_B \sim \Gamma_0. \quad (40)$$

This is equivalent with the condition that the first Landau level is shifted onto $\varepsilon = 0$, or $|\Delta\varepsilon_1| \sim \hbar\omega_B$, as naturally expected. To focus on this critical behavior, we present in Fig. 4 the plots of the density of states and the magnetization for $W = 0.1$, where the condition (40) is achieved at $n_c \sim 20000$. We see that the structure of the Landau level $n = 0$ still survives at $n_c = 100$, and M/B deviates largely from χ around this region. Here the magnetization at $\varepsilon = 0$ roughly scales as $M \propto \sqrt{B}$. At $n_c = 10000$, the gap collapses and the magnetization peak almost reaches that of χ , and thus $M \propto B$. If we fix the Fermi energy at $\varepsilon = 0$ and start the magnetic field from 0, the magnetization should exhibit the crossover from linear to square behavior in B .

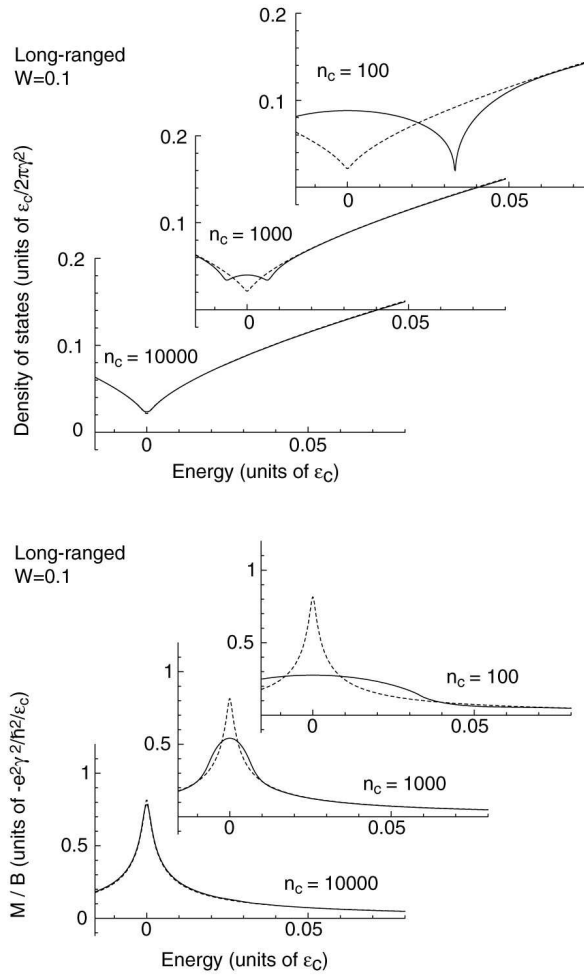


FIG. 4: Density of states (above) and the magnetization at $T = 0$ (below) in the long-ranged disorder with $W = 0.1$, in several magnetic fields. Dashed curves show the zero-field limit.

IV. DISCUSSION AND CONCLUSION

At nonzero temperatures, the magnetization as a function of the Fermi energy, $M(\varepsilon)$, is smoothed in accordance with (30), so that fine structures smaller than $k_B T$ are smeared out. This effect competes with energy broadening due to the impurity scattering, denoted here as Γ . We expect the crossover from the high-field (magnetic oscillation) to low-field regime ($M = \chi B$) occurs when either of $k_B T$ or Γ exceeds the Landau level spacing $\Delta\varepsilon$. In a usual 2D metal with a constant level spacing, it is known that the disorder effects can be effectively included as the Dingle temperature, $k_B T_D = \Gamma/\pi$. The reduction of the magnetic oscillation in disordered graphenes was studied with a constant Γ and discussed with respect to the Dingle temperature¹³.

In the realistic samples used in the experiment, dominant scatterers are supposed to be screened charged impurities.^{20,21,22} There the scattering matrix elements

between the states on a Fermi surface are proportional to $1/k_F$, not a constant like in our simple model. This situation is effectively modeled in our calculation by assuming that the parameter W depends on ε_F as $W \propto 1/\varepsilon_F^2$ in the long-range model. Then we expect that the susceptibility in the Boltzmann limit (36) becomes $\chi \propto 1/\varepsilon_F^3$. From the experimental value of the mobility of monolayer graphene, we estimate $W \sim 70/\varepsilon_F^2$ where ε_F is measured in units of meV.

The magnetization becomes highly singular at zero energy in our model, because the energy broadening, Γ_0 , is exponentially small here. In the case of charged impurities, however, the scattering rate at zero energy may not be small since the screening effect is strongly suppressed due to the lack of the density of states.^{21,22} We need a self-consistent calculation including the screening and the disorder to study such a case. This is out of the scope of this paper and left for a future study.

The experimental measurements of the magnetization of two-dimensional electron systems were performed on the semiconductor heterostructures, by using the superconducting quantum interference device (SQUID)^{23,24} or using the torque magnetometer.^{25,26,27,28} We expect that the detection of the grapheme magnetism is also feasible with those techniques.

To summarize, we have studied the magnetization in graphene monolayer in presence of the disorder with the effective mass model and the self-consistent Born approximation. The susceptibility $\chi(\varepsilon_F)$ has a sharp diamagnetic peak around zero energy even in the disorder, and a long tail proportional to the inverse of the Fermi energy. We have demonstrated that with the decrease of the magnetic field, the magnetic oscillation vanishes, and M/B converges to χ as the Landau gaps are smeared out.

ACKNOWLEDGMENTS

This work has been supported in part by the 21st Century COE Program at Tokyo Tech “Nanometer-Scale Quantum Physics” and by Grants-in-Aid for Scientific Research from the Ministry of Education, Culture, Sports, Science and Technology, Japan.

Note added in proof: — After completion of this work, we became aware of related work, Ref. 30.

APPENDIX A: SUSCEPTIBILITY

We present here the derivation of the susceptibility in SCBA for the short-ranged disorder Eq. (32) and for the long-ranged (38). For the short-ranged case, we obtain from (13) and (29),

$$\chi = -\frac{g_v g_s}{2\pi^2 \gamma^2 W} \int_{-\infty}^{\infty} d\varepsilon f(\varepsilon) \int_{-\infty}^{\varepsilon} d\varepsilon' \text{Im} \left. \frac{\partial^2 \Sigma(\varepsilon', B)}{\partial B^2} \right|_{B=0}. \quad (\text{A1})$$

Let us introduce a variable $X = \varepsilon - \Sigma$ to write Σ as a function (X, B) as

$$\Sigma(\varepsilon, B) \equiv \tilde{\Sigma}(X, B) = \frac{W(\hbar\omega_B)^2}{2} \sum_{n=-\infty}^{\infty} \frac{g(\varepsilon_n)}{X - \varepsilon_n}. \quad (\text{A2})$$

Using $\frac{\partial \Sigma}{\partial B} = -\frac{\partial X}{\partial B}$, the derivative of Σ can be written in terms of those of $\tilde{\Sigma}$ as

$$\frac{\partial \Sigma(\varepsilon, B)}{\partial B} = \left[1 + \frac{\partial \tilde{\Sigma}(X, B)}{\partial X} \right]^{-1} \frac{\partial \tilde{\Sigma}(X, B)}{\partial B}. \quad (\text{A3})$$

The second-order derivative can be derived similarly as

$$\begin{aligned} \frac{\partial^2 \Sigma}{\partial B^2} &= \left(1 + \frac{\partial \tilde{\Sigma}}{\partial X} \right)^{-1} \times \\ &\left[\frac{\partial^2 \tilde{\Sigma}}{\partial B^2} - 2 \frac{\partial^2 \tilde{\Sigma}}{\partial X \partial B} \left(\frac{\partial \Sigma}{\partial B} \right) + \frac{\partial^2 \tilde{\Sigma}}{\partial X^2} \left(\frac{\partial \Sigma}{\partial B} \right)^2 \right]. \end{aligned} \quad (\text{A4})$$

Equation (A2) can be explicitly written as

$$\tilde{\Sigma}(X, B) = \frac{W}{2} \Delta t \left[\frac{h(0)}{2} + \sum_{n=1}^{\infty} h(n\Delta t) \right], \quad (\text{A5})$$

where $\Delta t = (\hbar\omega_B)^2 = 2\gamma^2 eB/\hbar$, and $h(x) = 2Xg(\sqrt{X})/(X^2 - t)$

When $|\text{Im}X| \gg \hbar\omega_B$, $h(t)$ is regarded as smooth with respect to increment Δt , and we can use an approximation

$$\begin{aligned} \Delta t \left[\frac{h(0)}{2} + \sum_{0 < n < \infty} h(n\Delta t) \right] &= \\ \int_0^\infty h(t) dt - \frac{(\Delta t)^2}{12} \left[h'(0) + \frac{1}{2} h'(\infty) \right], \end{aligned} \quad (\text{A6})$$

where $O(\Delta t^3)$ is neglected. Then we have

$$\tilde{\Sigma}(X, B) - \tilde{\Sigma}(X, 0) = -\frac{W}{24} h'(0)(\Delta t)^2 \quad (\text{A7})$$

which leads to

$$\frac{\partial \tilde{\Sigma}}{\partial B} \Big|_{B=0} = 0 \quad (\text{A8})$$

$$\frac{\partial^2 \tilde{\Sigma}}{\partial B^2} \Big|_{B=0} = -\frac{W}{6} \left(\frac{2e\gamma^2}{\hbar} \right)^2 \frac{1}{X^3}. \quad (\text{A9})$$

With (A1), (A3), and (A4), we obtain

$$\begin{aligned} \chi &= \frac{g_v g_s e^2 \gamma^2}{3\pi^2} \int_{-\infty}^{\infty} d\varepsilon f(\varepsilon) \\ &\times \text{Im} \int_{-\infty}^{\varepsilon} d\varepsilon' \left(1 + \frac{\partial \tilde{\Sigma}'}{\partial X'} \right)^{-1} \frac{1}{X'^3} \Big|_{B=0}, \end{aligned} \quad (\text{A10})$$

where $\tilde{\Sigma}'$ and X' are functions of ε' . Integration in ε' can be executed with the aid of

$$d\varepsilon' = \left(1 + \frac{\partial \tilde{\Sigma}'}{\partial X'} \right) dX', \quad (\text{A11})$$

and finally obtain

$$\chi = -\frac{g_v g_s e^2 \gamma^2}{6\pi^2} \frac{1}{\hbar^2} \int_{-\infty}^{\infty} d\varepsilon f(\varepsilon) \text{Im} \frac{1}{X^2} \Big|_{B=0}, \quad (\text{A12})$$

which is (32). We can derive the identical equation starting from the general formula based on the linear response theory²⁹.

We can show that the susceptibility in the present system has a ‘sum rule’, where the integration of $\chi(\mu)$ over μ is a constant independent of the disorder strength. From (A12), we have

$$\begin{aligned} \int_{-\infty}^{\infty} \chi(T, \mu) d\mu &= \int_{-\infty}^{\infty} \chi(0, \varepsilon) d\varepsilon \\ &= -\frac{g_v g_s e^2 \gamma^2}{6\pi^2} \frac{1}{\hbar^2} \int_{-\infty}^{\infty} d\varepsilon \int_{-\infty}^{\varepsilon} d\varepsilon' \text{Im} \frac{1}{X'^2} \Big|_{B=0} \\ &= -\frac{g_v g_s e^2 \gamma^2}{6\pi^2} \frac{1}{\hbar^2} \int_{-\infty}^{\infty} d\varepsilon \varepsilon \text{Im} \frac{1}{X^2} \Big|_{B=0}. \end{aligned} \quad (\text{A13})$$

By replacing the integrating variable ε with X , this becomes

$$\begin{aligned} \int_{-\infty}^{\infty} \chi d\mu &= -\frac{g_v g_s e^2 \gamma^2}{6\pi^2} \frac{1}{\hbar^2} \frac{1}{2i} \oint_C dX \left(1 + \frac{\partial \tilde{\Sigma}}{\partial X} \right) \frac{\tilde{\Sigma} + X}{X^2} \\ &= -\frac{g_v g_s e^2 \gamma^2}{6\pi^2} \frac{1}{\hbar^2} \frac{1}{2i} \oint_C \frac{1}{X} = -\frac{g_v g_s e^2 \gamma^2}{6\pi} \frac{1}{\hbar^2} \end{aligned} \quad (\text{A14})$$

where integration path C is a circle with an infinite radius with clockwise direction, and we used $\tilde{\Sigma} \sim O(1/X)$ for large $|X|$.

The susceptibility for the long-ranged disorder (38) can be derived in a similar way to the short-ranged case, while the procedure is rather complicated. From (24) and (29), we obtain

$$\begin{aligned} \chi &= -\frac{g_v g_s}{2\pi^2 \gamma^2 W} \int_{-\infty}^{\infty} d\varepsilon f(\varepsilon) \int_{-\infty}^{\varepsilon} d\varepsilon' \\ &\quad \text{Im} \frac{1}{2} \frac{\partial^2}{\partial B^2} (\Sigma^+(\varepsilon', B) + \Sigma^-(\varepsilon', B)) \Big|_{B=0} \end{aligned} \quad (\text{A15})$$

We introduce a variable $X^\pm = \varepsilon - \Sigma^\pm$ and define $\Sigma^\pm \equiv \tilde{\Sigma}^\pm(X^+, X^-, B)$, with

$$\tilde{\Sigma}^+ \equiv W(\hbar\omega_B)^2 \sum_{n=0}^{\infty} \frac{X^- g(\varepsilon_n)}{X^+ X^- - \varepsilon_n^2} \quad (\text{A16})$$

$$\tilde{\Sigma}^- \equiv W(\hbar\omega_B)^2 \sum_{n=1}^{\infty} \frac{X^+ g(\varepsilon_n)}{X^+ X^- - \varepsilon_n^2}. \quad (\text{A17})$$

The derivatives of Σ can be written in terms of $\tilde{\Sigma}$ as

$$\frac{\partial \Sigma^i}{\partial B} = A_{ij} \frac{\partial \tilde{\Sigma}^j}{\partial B}, \quad (\text{A18})$$

and

$$\frac{\partial^2 \Sigma^i}{\partial B^2} = A_{ij} \left(\frac{\partial^2 \tilde{\Sigma}^j}{\partial B^2} - 2 \frac{\partial^2 \tilde{\Sigma}^j}{\partial X^k \partial B} \frac{\partial \Sigma^k}{\partial B} + \frac{\partial^2 \tilde{\Sigma}^j}{\partial X^k \partial X^l} \frac{\partial \Sigma^k}{\partial B} \frac{\partial \Sigma^l}{\partial B} \right), \quad (\text{A19})$$

where $i, j, k, l = \pm$, repeated indices indicate summation, and the matrix A is defined as

$$(A^{-1})_{ij} \equiv \delta_{ij} + \frac{\partial \tilde{\Sigma}^i}{\partial X^j}. \quad (\text{A20})$$

We can calculate the derivatives of $\tilde{\Sigma}^\pm$ at $B = 0$ in a similar way to the short-ranged case, and then obtain those for Σ^\pm through Eqs. (A18) and (A19). As a result, we have

$$\begin{aligned} \frac{\partial^2}{\partial B^2} (\Sigma^+ + \Sigma^-) \Big|_{B=0} &= \frac{1}{1 + \alpha + 2\beta} \left(\frac{2e\gamma^2}{\hbar} \right)^2 \frac{1}{X^3} \\ &\times \left(-\frac{W}{6} + \frac{1}{1 - \alpha} \frac{W^2}{2} - \frac{2\beta}{(1 - \alpha)^2} \frac{W^2}{4} \right), \end{aligned} \quad (\text{A21})$$

where $X \equiv \lim_{B \rightarrow 0} X^+ = \lim_{B \rightarrow 0} X^-$, and

$$\alpha = 2W \int_0^\infty t dt \frac{g(t)}{X^2 - t^2}, \quad (\text{A22})$$

$$\beta = 2W \int_0^\infty t dt \frac{-X^2 g(t)}{(X^2 - t^2)^2}. \quad (\text{A23})$$

Substituting (A21) in (A15), this becomes

$$\chi = -\frac{g_v g_s e^2 \gamma^2}{6\pi^2 \hbar^2} \int_{-\infty}^\infty d\varepsilon f(\varepsilon) \int_{X(-\infty)}^{X(\varepsilon)} dX' \times \text{Im} \frac{1}{X'^3} \left[-1 + 3W \left(\frac{1}{1 - \alpha'} - \frac{\beta'}{(1 - \alpha')^2} \right) \right], \quad (\text{A24})$$

where α' and β' have the argument X' for X in (A22) and (A23), and the integration in ε' has been replaced by $d\varepsilon' = (1 + \alpha' + \beta')dX'$.

In the region $|\varepsilon| \ll \varepsilon_c$, (A22) and (A23) can be approximately written as $\alpha \approx -W \log(-\varepsilon_c^2/X^2)$ and $\beta \approx W$. By substituting them in (A24), we can execute the integration in X' to obtain Eq. (38). Here the expression of the integrand is valid only for $|\varepsilon| \ll \varepsilon_c$ while the integration runs over all ε , but this is justified since the integral converges.

¹ K. S. Novoselov, A. K. Geim, S. V. Morozov, D. Jiang, Y. Zhang, S. V. Dubonos, I. V. Grigorieva, and A. A. Firsov, *Science* **306**, 666 (2004).

² C. Berger, Z. Song, T. Li, X. Li, A. Y. Ogbazghi, R. Feng, Z. Dai, A. N. Marchenkov, E. H. Conrad, P. N. First, and W. A. de Heer, *J. Phys. Chem. B* **108**, 19912 (2004).

³ K. S. Novoselov, A. K. Geim, S. V. Morozov, D. Jiang, M. I. Katsnelson, I. V. Grigorieva, S. V. Dubonos, and A. A. Firsov, *Nature* **438**, 197 (2005).

⁴ Y. Zhang, Y. W. Tan, H. L. Stormer, and P. Kim, *Nature* **438**, 201 (2005).

⁵ J. W. McClure, *Phys. Rev.* **104**, 666 (1956).

⁶ M. P. Sharma, L. G. Johnson, and J. W. McClure, *Phys. Rev. B* **9**, 2467 (1974).

⁷ S. A. Safran and F. J. DiSalvo, *Phys. Rev. B* **20**, 4889 (1979).

⁸ J. Blinowski and C. Rigaux, *J. Phys. (Paris)* **45**, 545 (1984).

⁹ R. Saito and H. Kamimura, *Phys. Rev. B* **33**, 7218 (1986).

¹⁰ N. H. Shon and T. Ando, *J. Phys. Soc. Jpn.* **67**, 2421 (1998).

¹¹ Y. Zheng and T. Ando, *Phys. Rev. B* **65**, 245420 (2002).

¹² T. Ando, Y. Zheng, and H. Suzuura, *J. Phys. Soc. Jpn.* **71**, 1318 (2002).

¹³ S. G. Sharapov, V. P. Gusynin, and H. Beck, *Phys. Rev. B* **69**, 075104 (2004).

¹⁴ V. P. Gusynin and S. G. Sharapov, *Phys. Rev. B* **71**, 125124 (2005).

¹⁵ V. P. Gusynin and S. G. Sharapov, *Phys. Rev. B* **73**, 245411 (2006).

¹⁶ N. M. R. Peres, F. Guinea, and A. H. Castro Neto, *Phys. Rev. B* **73**, 125411 (2006).

¹⁷ M. Igami, T. Nakanishi, and T. Ando, *J. Phys. Soc. Jpn.* **68**, 716 (1999); *ibid* **68**, 3146 (1999); *ibid* **70**, 481 (2001).

¹⁸ T. Ando, T. Nakanishi, and M. Igami, *J. Phys. Soc. Jpn.* **68**, 3994 (1999).

¹⁹ V. M. Pereira, F. Guinea, J. M. B. Lopes dos Santos, N. M. R. Peres, and A. H. Castro Neto, *Phys. Rev. Lett.* **96**, 036801 (2006).

²⁰ K. Nomura and A. H. MacDonald, *Phys. Rev. Lett.* **96**, 256602 (2006).

²¹ T. Ando, *J. Phys. Soc. Jpn.*, **75**, 74716 (2006).

²² K. Nomura and A. H. MacDonald, *Phys. Rev. Lett.* **98**, 076602 (2007).

²³ H. L. Stormer, T. Haavasoja, V. Narayanamurti, A. C. Gossard, and W. Wiegmann, *J. Vac. Sci. Technol. B* **1**, 423 (1983).

²⁴ I. Meinel, D. Grundler, S. Bargst adt-Franke, C. Heyn, and D. Heitmann, *Appl. Phys. Lett.* **70**, 3305 (1997).

²⁵ J. P. Eisenstein, H. L. Stormer, V. Narayanamurti, A. Y. Cho, A. C. Gossard, and C. W. Tu, *Phys. Rev. Lett.* **55**, 875 (1985).

²⁶ A. Potts, R. Shepherd, W. G. Herrenden-Harker, M. Elliott, C. L. Jones, A. Usher, G. A. C. Jones, D. A. Ritchie, E. H. Linfield, and M. Grimshaw, *J. Phys. C* **8**, 5189 (1996).

²⁷ S. A. J. Wiegers, M. Specht, L. P. Levy, M. Y. Simmons, D. A. Ritchie, A. Cavanna, B. Etienne, G. Martinez, and P. Wyder, *Phys. Rev. Lett.* **79**, 3238 (1997).

²⁸ M. Zhu, A. Usher, A. J. Matthews, A. Potts, M. Elliott, W.

G. Herrenden-Harker, D. A. Ritchie, and M. Y. Simmons, Phys. Rev. B **67**, 155329 (2003).
²⁹ H. Fukuyama, Prog. Theor. Phys. **45**, 704 (1971).
³⁰ H. Fukuyama, J. Phys. Soc. Jpn. **76**, 043711 (2007).